Supporting Information

Steam Reforming of Methane by Titanium oxide Photocatalysts with Hollow Spheres

Akira Yamaguchi[*], *Tomoki Kujirai, Takeshi Fujita, Hideki Abe, and Masahiro Miyauchi*[*]

Table of Contents

1. Calculation of the outer quantum efficiency

Outer quantum efficiency for Rh/hollow TiO_2/Pt was calculated by the amount of hydrogen production divided by irradiated photon numbers determined by the spectrum of the light source.

$$outer\ quantum\ efficiency\ [\%] = \frac{amount\ of\ consumed\ electrons\ to\ produce\ H_2[s^{-1}]}{irradiated\ photon\ number\ [s^{-1}]} = \frac{2 \cdot H\ [mol\ s^{-1}] \cdot N_A[mol^{-1}]}{\sum_{\lambda=200}^{800} \frac{E(\lambda)[\mu W \cdot cm^{-2}] \cdot A[cm^2] \cdot 10^{-6}}{h[J \cdot s] \cdot c[m \cdot s^{-1}]/\lambda[nm]}}$$

$H[mol\ s^{-1}]$: Hydrogen production rate

$N_A[mol^{-1}]$: Avogadro number (6.02×10^{23})

$E(\lambda)[\mu W \cdot cm^{-2}]$: Light energy when the wavelength is λ nm

h[J·s]: Planck constant(= 6.63×10^{-34})

$c[m \cdot s^{-1}]$: Speed of light (= 3.0×10^{8})

$\lambda[nm]$: Wavelength

$A[cm^2]$: Light irradiated area (= 0.175 cm^2)

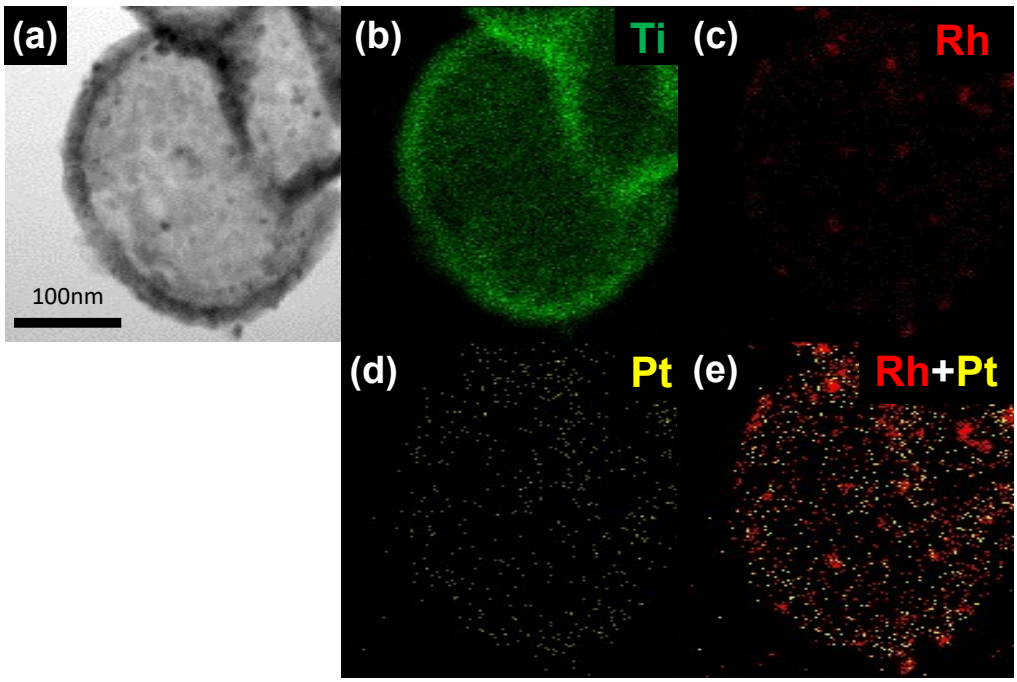

Figure S1. (a) FE-TEM image and (b-e) elemental mapping of the Rh/hollow TiO_2/Pt photocatalyst.

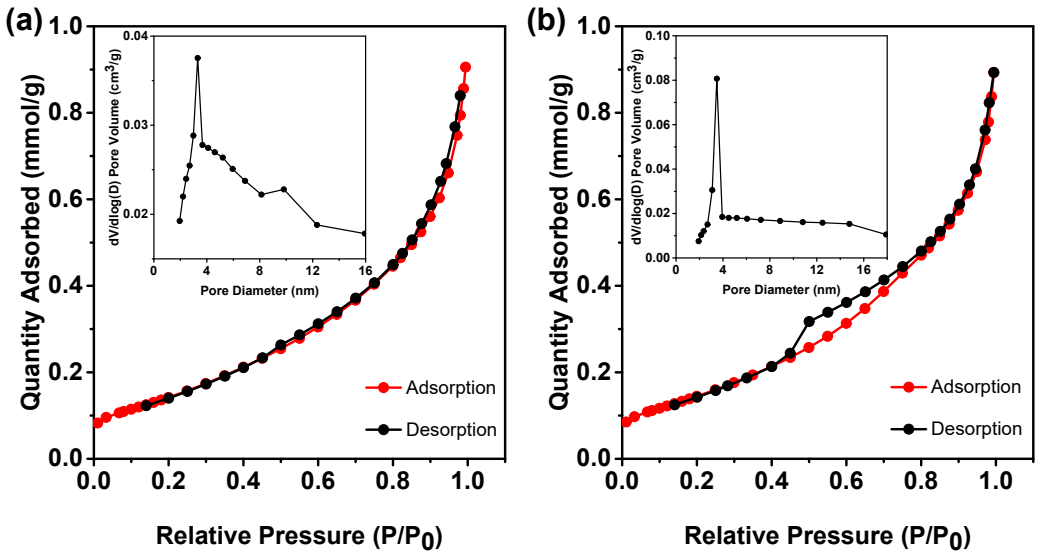

Figure S2. N_2 adsorption-desorption isotherm of (a) hollow TiO_2 and (b) Rh/hollow TiO_2/Pt. The inset shows the pore size distribution.

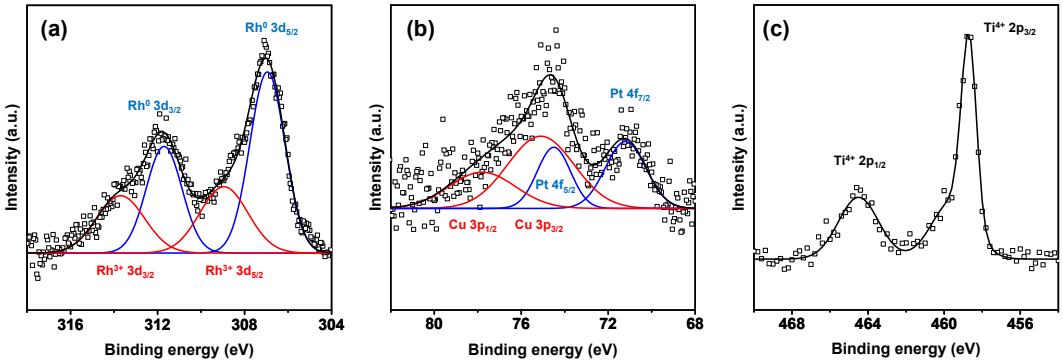

Figure S3. XPS spectra of Rh/hollow TiO_2/Pt for the (a) Rh 3d, (b) Pt 4f, and (c) Ti 2p regions. The Cu 3p peaks in panel (b) originated from the Cu tape used to fix the sample on the instrument holder.

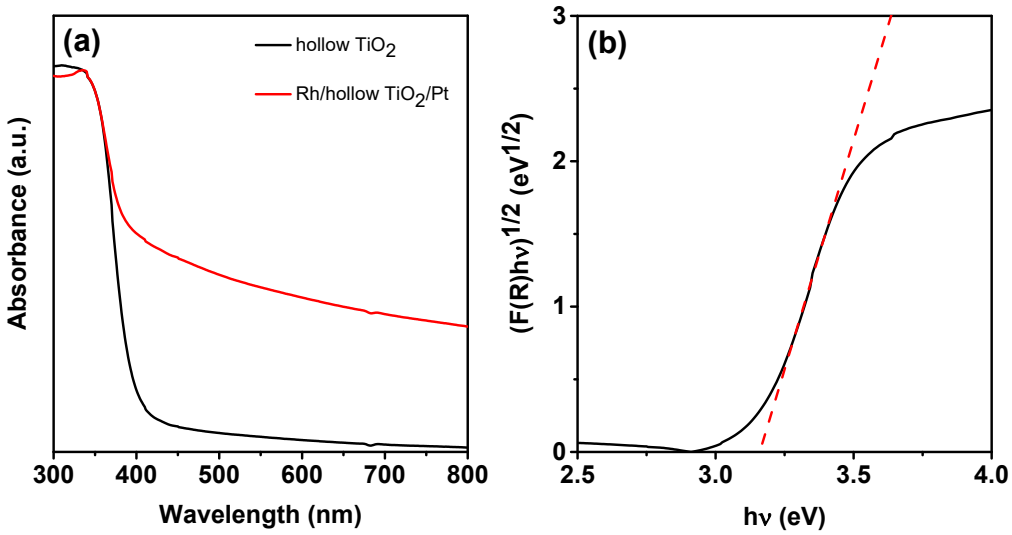

Figur
e S4. Optical properties of hollow TiO_2 (black line) and Rh/hollow TiO_2/Pt (red line). (a) UV-Vis spectra and (b) the corresponding Tauc-plot.

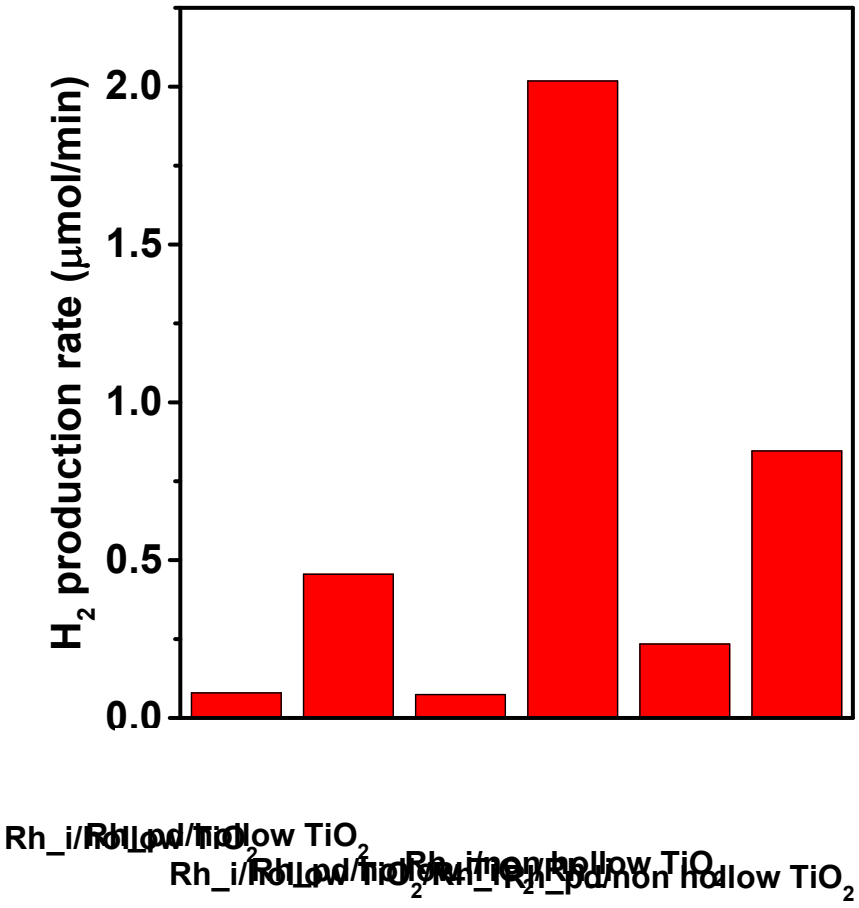

Figure S5. Photocatalytic SRM activity comparison between hollow sphere-structured TiO_2 and non-hollow TiO_2 loaded with Rh as a co-catalyst. The operation temperature was 300 ℃.

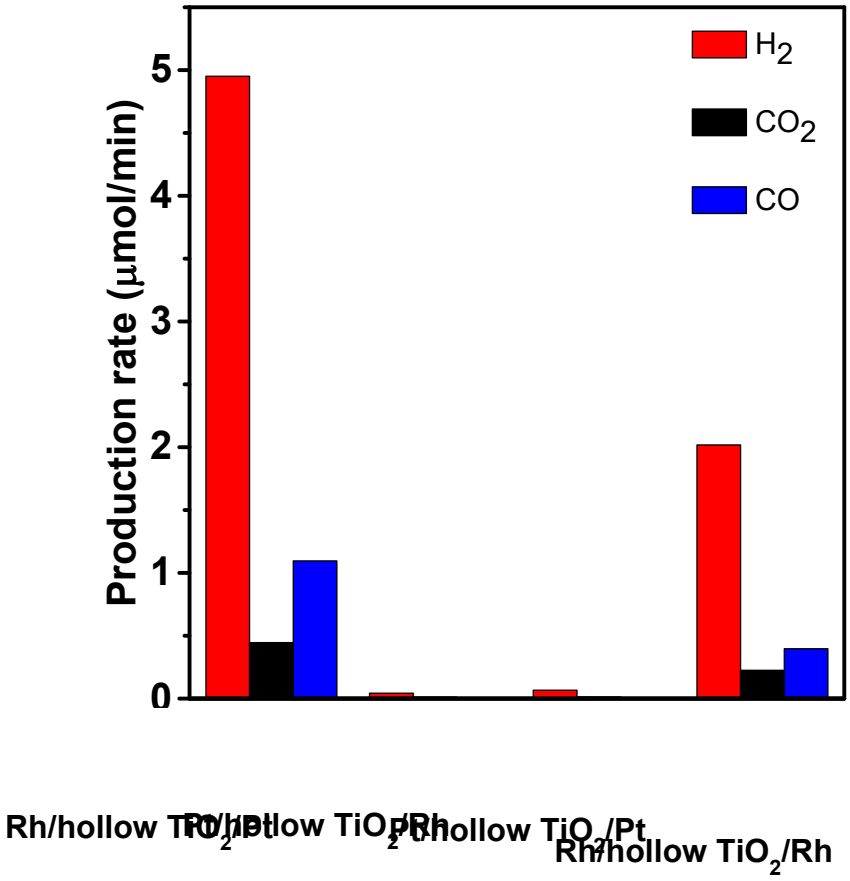

Figure S6. Product distribution generated by Pt and Rh-loaded hollow TiO_2 photocatalysts during SRM. The operation temperature was 300 ℃.

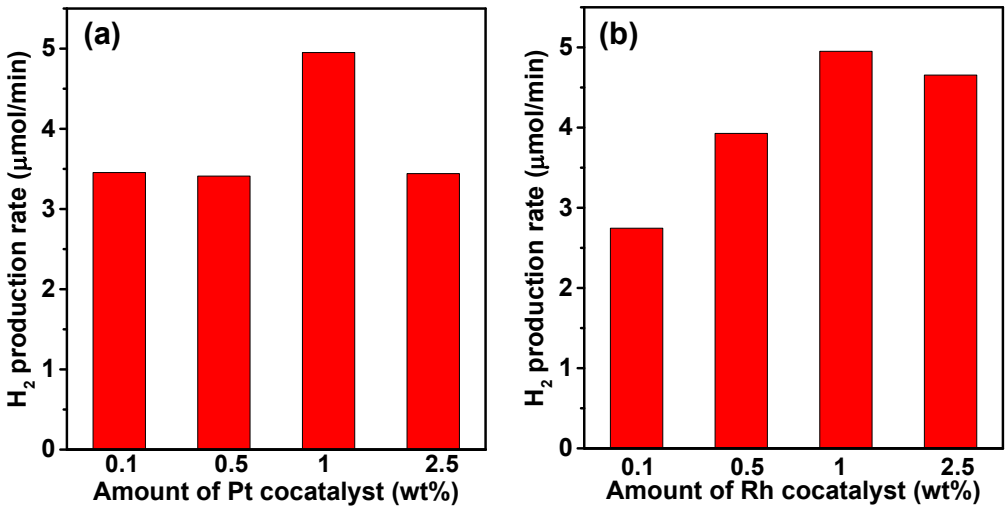

Figure S7. Influence of co-catalyst loading amount of photocatalytic SRM activity on Rh/hollow TiO_2/Pt. (a) The Pt loading amount was varied between 0.1 and 2.5 wt% at a constant Rh amount to 1 wt%. (b) The Rh loading amount was varied between 0.1 and 2.5 wt% at a constant Pt amount to 1 wt%. The operation temperature was 300 ℃.

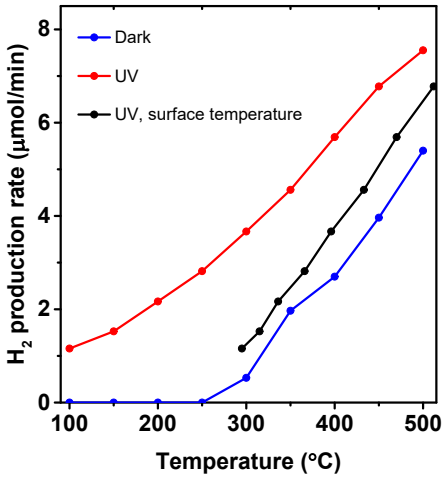

Figure S8. Temperature dependence of photocatalytic SRM activity on Rh/hollow TiO_2/Pt under dark (blue line) and UV irradiation (red line) conditions. The black line represents the H_2 production rate under UV irradiation at the surface temperature, not operation temperature.

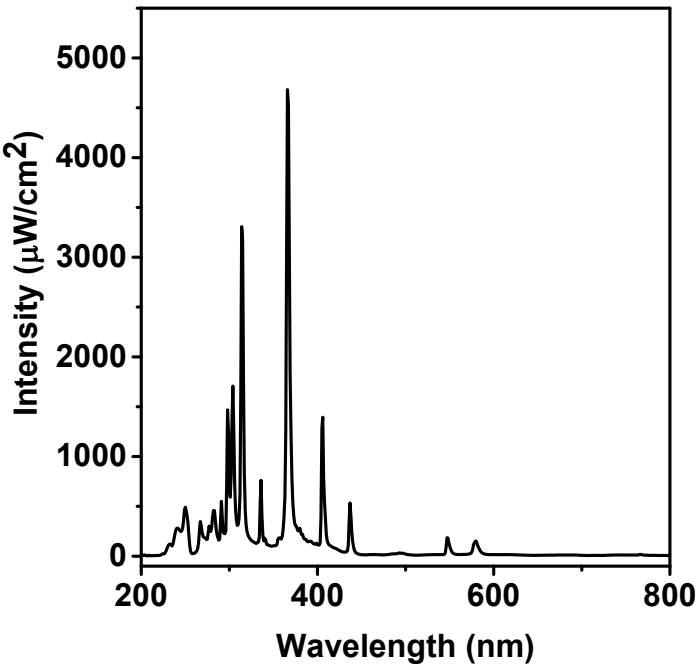

Figure S9. Spectrum of the Hg-Xe lamp used for the SRM test.

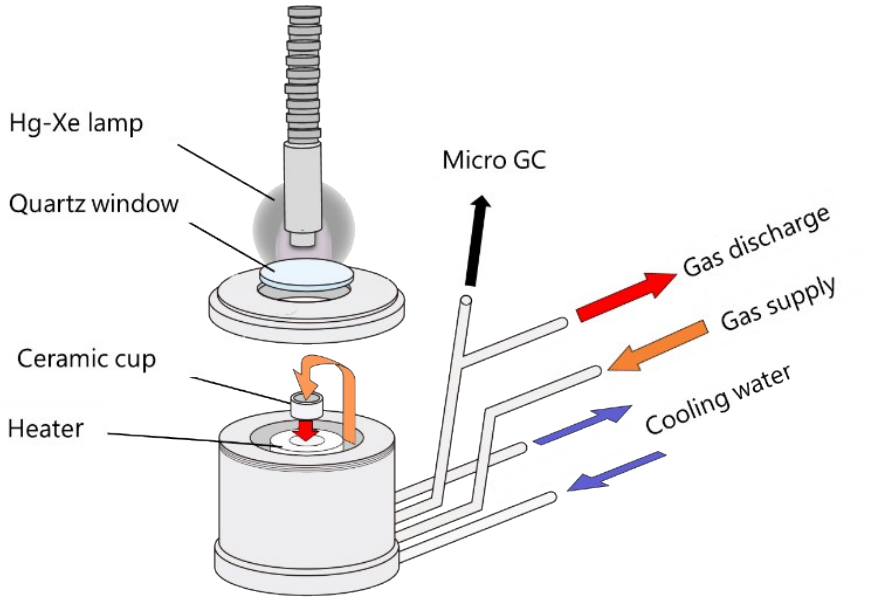

Figure S10. Schematic image of the flow-reactor used for SRM test. In this setup, the sample was mounted in the ceramic cup and placed in the reactor equipped with a heater. Reactant gas was introduced to the reactor and reaction product was analyzed with online-connected micro-GC. The UV lamp was irradiated through quartz window at the upper part of the reactor.

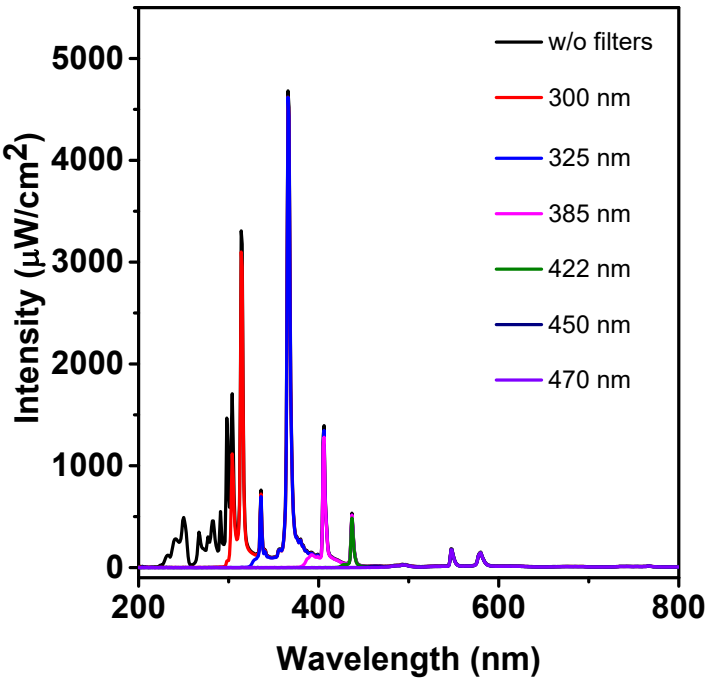

Figure S11. Spectrum of the Hg-Xe lamp obtained using long-pass cutoff filters. The cutoff wavelength for each filter is indicated.